Lithos 294–295 (2017) 412–417

Contents lists available at ScienceDirect

Lithos

journal homepage: www.elsevier.com/locate/lithos

Letter

Graphite–$(Mo,W)S_2$ intergrowth as a palaeoenvironmental proxy in metasedimentary rocks

Alexandre Raphael Cabral [a,b,*], Armin Zeh [c], Nívea Cristina da Silva Viana [d], Thomas Schirmer [e], Bernd Lehmann [f]

[a] Centro de Pesquisas Professor Manoel Teixeira da Costa (CPMTC), Instituto de Geociências, Universidade Federal de Minas Gerais (UFMG), Av. Antônio Carlos 6.627, 31270-901 Belo Horizonte, MG, Brazil
[b] Centro de Desenvolvimento da Tecnologia Nuclear (CDTN), Av. Antônio Carlos 6.627, 31270-901 Belo Horizonte, MG, Brazil
[c] Institut für Angewandte Geowissenschaften, Mineralogie und Petrologie, Karlsruher Institut für Technologie (KIT), Adenauerring 20b, Geb. 50.40, 76131 Karlsruhe, Germany
[d] Vale Manganês S.A., Rua Duque de Caxias s/n, Morro da Mina, 36400-000 Conselheiro Lafaiete, MG, Brazil
[e] Institute of Disposal Research, Technische Universität Clausthal, Adolph-Roemer-Str. 2a, 38678 Clausthal-Zellerfeld, Germany
[f] Mineral Resources, Technische Universität Clausthal, Adolph-Roemer-Str. 2a, 38678 Clausthal-Zellerfeld, Germany

ARTICLE INFO

Article history:
Received 12 July 2017
Accepted 1 October 2017
Available online 13 October 2017

Keywords:
Tungsten-bearing molybdenite
Graphite
Molybdenum proxy
Queluzite
Barbacena greenstone belt
Minas Gerais

ABSTRACT

Molybdenum enrichment in pristine organic-C-rich sedimentary rocks forms the basis for inferring the presence of dissolved oxygen in seawater. Organic matter removes dissolved hexavalent Mo from seawater where anoxic and euxinic conditions are attained. However, it is unknown whether this Mo-based proxy is retained under metamorphic conditions where organic C is no longer preserved. Here, we describe aggregates of graphite and molybdenite (MoS_2) containing up to 21 mass per cent of W as tungstenite (WS_2) in solid solution. These aggregates are disseminated in a sulfide-rich Mn-silicate-carbonate rock (queluzite), metamorphosed under amphibolite-facies conditions within the Archaean Barbacena greenstone belt in Minas Gerais, Brazil. Our finding indicates that: (i) W is, like Mo, a palaeoenvironmental proxy; (ii) the W proxy is sensitive to high fS_2/fO_2 environments; (iii) both Mo and W proxies survive amphibolite-facies overprint as $(Mo,W)S_2$ intergrown with graphite. Archaean greenstones are potential candidates for storing palaeoenvironmental information as $(Mo,W)S_2$–graphite intergrowths.

1. Introduction

Molybdenite (MoS_2) is the most important ore mineral of molybdenum and occurs in a variety of ore deposits associated with felsic igneous rocks. The mineral is isostructural with tungstenite (WS_2) and a complete solid solution between them exists in the synthetic system Mo–W–S (Moh and Udubasa, 1976). In more complex systems involving silicate melts, Mo is fractionated from W in response to variations in fugacity (f) of oxygen and sulfur, and to the preference of Mo to form its own sulfide (Candela and Bouton, 1990; Lodders and Palme, 1991; Mengason et al., 2011). In fact, "Mo in nature is mostly found as a sulfide, while W is usually found in the form of oxygen compounds" (Goldschmidt, 1954). This fractionation is also expressed in the general lack of W accommodated as WS_2 in molybdenite. Where detected in molybdenite, W can be ascribed to analytical interference from tungstate minerals (Höll and Weber-Diefenbach, 1973; Pašava et al., 2016). Only a few examples of limited solid solution of tungstenite in molybdenite have adequately been recorded, all in association with igneous rocks (Barkov et al., 2000; Pašava et al., 2015; Silva et al., 2015), attaining up to about 6 mass per cent (%) of W in molybdenite (Barkov et al., 2000). It thus seems that magmatic-hydrothermal environments rarely reach the high fS_2/fO_2 conditions that are necessary for an extensive solid-solution series between molybdenite and tungstenite, and/or that W is already removed – that is, fractionated – from the magmatic-hydrothermal system at the time of molybdenite precipitation.

Precipitation of MoS_2 not only occurs in magmatic-hydrothermal systems, but also in organic-rich sedimentary rocks that accumulated in anoxic and euxinic environments (Helz et al., 1996; Kao et al., 2001). In such rocks, S-rich organic matter is capable of capturing Mo soluble as molybdate in seawater where a threshold concentration of H_2S is reached (Helz et al., 1996; Tribovillard et al., 2004). Organic-matter trapping of W soluble as tungstate in seawater may take place in a similar way, in form of thiotungstate, but it requires H_2S concentrations that are two orders of magnitude higher than those needed for Mo fixation as thiomolybdate (Mohajerin et al., 2016). Accordingly, uptake of both Mo and W by organic matter in seawater is possible if the fS_2/fO_2

* Corresponding author at: Centro de Pesquisas Professor Manoel Teixeira da Costa (CPMTC), Instituto de Geociências, Universidade Federal de Minas Gerais (UFMG), Av. Antônio Carlos 6.627, 31270-901 Belo Horizonte, MG, Brazil.
E-mail address: alexandre.cabral@tu-clausthal.de (A.R. Cabral).

https://doi.org/10.1016/j.lithos.2017.10.007
0024-4937/

ratio is sufficiently high. Conversely, the occurrence of W-rich MoS_2, a solid solution between WS_2 and MoS_2, in ancient black-shale deposits has the ability to provide information about seawater fS_2/fO_2. Here, we describe for the first time WS_2-rich molybdenite from a metamorphosed sedimentary deposit formed in a black-shale environment within an Archaean greenstone belt. This finding suggests that WS_2-rich molybdenite intergrown with graphite represents a mineralogical proxy for a "whiff of oxygen" (Anbar et al., 2007), which would otherwise be obscured by greenstone-belt metamorphism.

2. Geological setting and sample material

We examined samples of a Mn-silicate-carbonate rock, queluzite (Derby, 1901, 1908), from the Morro da Mina mine near Conselheiro Lafaiete in Minas Gerais. The rock is part of a manganese-formation unit, the Lafaiete Formation, which is traceable for over 100 km (Ebert, 1957, 1962). The Lafaiete Formation consists of gondite, queluzite, graphite schist, quartzite and paragneiss. Gondite refers to a carbonate-free, Mn-silicate rock, whereas queluzite is a Mn-silicate rock containing carbonate (Dasgupta et al., 1990; see below). These rocks are part of the Barbacena greenstone belt (Pires, 1978), which is assumed to be of Archaean age. An Archaean depositional age of ~2.7 Ga for the Lafaiete Formation has been suggested on the basis of stratigraphic correlation with the Rio das Velhas greenstone belt in the Quadrilátero Ferrífero to the north (Fig. 1; Herz and Banerjee, 1973; see Baltazar and Zucchetti, 2007, for age constraints on the Rio das Velhas greenstone belt). Recently, another greenstone-belt sequence, Pitangui, to the northwest of the Quadrilátero Ferrífero (Fig. 1), has had its stratigraphic correlation with the Rio das Velhas greenstone belt corroborated with geochronological data (Soares et al., 2017). An Archaean age for Pitangui lends support to the correlation between the Lafaiete Formation and the Nova Lima Group of the Rio das Velhas greenstone belt (Grossi Sad et al., 1983). The Barbacena greenstone belt was intruded by a tonalitic pluton during the Palaeoproterozoic at 2124 ± 2 Ma (zircon and titanite U–Pb age, Noce et al., 2000).

Queluzite is currently the main Mn-ore type at the Morro da Mina mine, which has been in operation since 1902. Queluzite orebodies are surrounded by quartz–biotite schist with intercalations of graphite schist, quartzite, garnet–amphibole schist and amphibolite. The latter contains the following mineral assemblage: hornblende, plagioclase (about An_{40}), garnet, biotite and clinozoisite (Herz and Banerjee, 1973), which indicate amphibolite facies of regional metamorphism. A minimum metamorphic temperature of 600 °C can be estimated on the basis of the assemblage rhodochrosite–tephroite–pyroxmangite found in queluzite (Peters et al., 1974). The Mn orebodies consist mostly of queluzite and subordinate gondite. The rock queluzite has an essential Mn-carbonate component, ubiquitous graphite and a variety of Mn-silicate minerals, such as spessartine, rhodonite, pyroxmangite and tephroite, whereas gondite is a Mn-silicate rock widely free of carbonate, the main silicate component of which is spessartine (Candia and Girardi, 1979; Derby, 1908; Guimarães, 1929; Hussak, 1906; Miller and Singewald, 1917; Pires, 1983; Viana, 2009), as well as disseminated alabandite, MnS (Park et al., 1951; Viana, 2009).

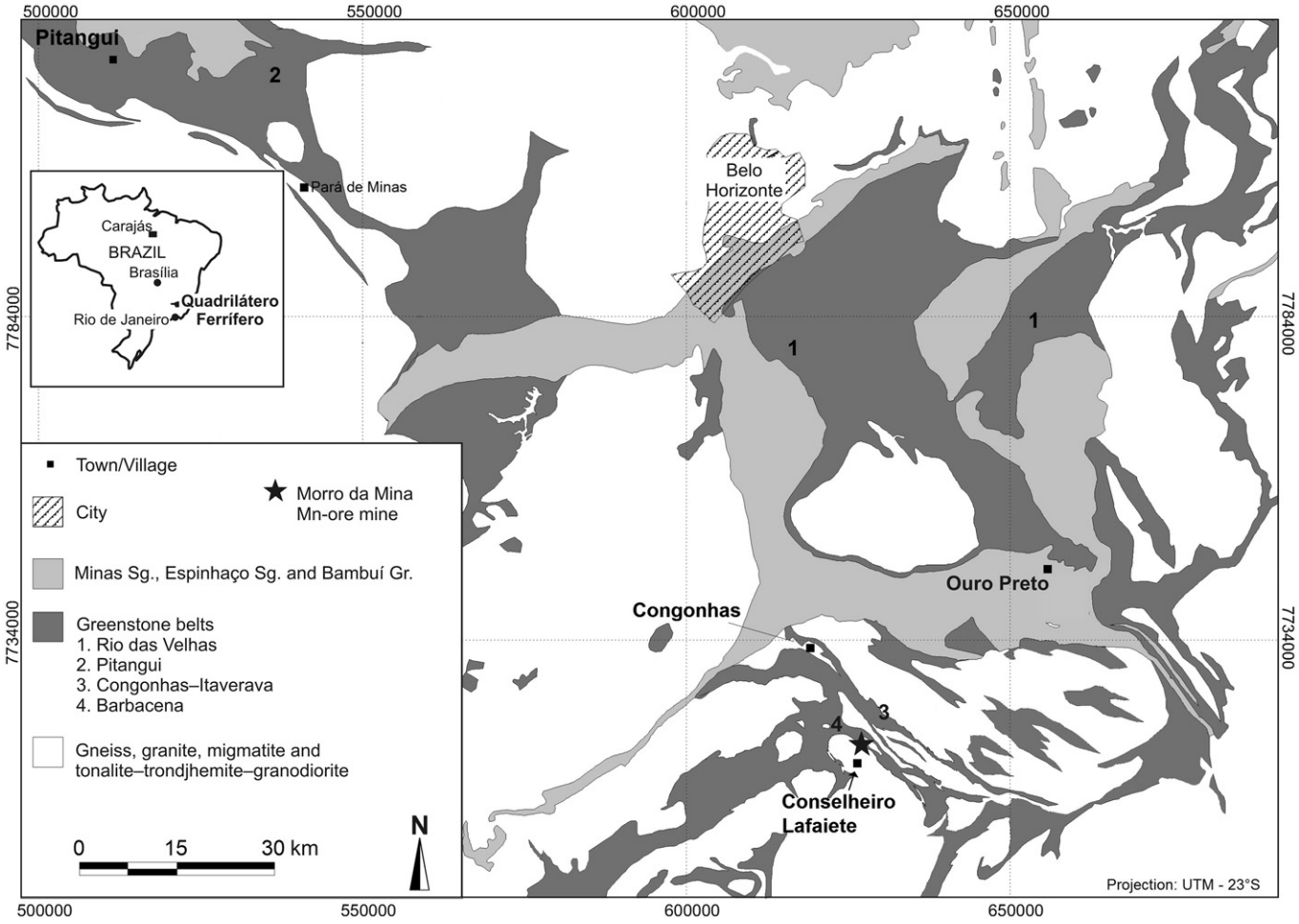

Fig. 1. Distribution of greenstone belts in the Quadrilátero Ferrífero and adjacent areas, and location of the Morro da Mina mine; geological outline as compiled from Dorr (1969) and Corrêa Neto et al. (2012). Sg. = Supergroup; Gr. = Group.

The rock succession of Morro da Mina experienced isoclinal folding and ductile shearing, the superposition of which resulted in a sigmoidal geometry of queluzite orebodies, reaching 100 m in thickness (Viana, 2009). Shear zones are marked by graphite schist. Its shear surfaces are prominently striated – that is, slicken striae developed on graphite-forming foliation. Massive veins of rhodonite, a few centimetres thick, occur in queluzite orebodies.

Our sample material is a collection of queluzite rocks from the ore stockpile of the Morro da Mina, hence the sample collection represents the run of mine. Seven (7) hand specimens of queluzite were selected for this study. The hand specimens look massive, but at close inspection a slight layering is discernible. The samples are fine in grain size and dark grey in colour, being easily scratched with the point of the pick. Two samples of graphite schist were added for whole-rock chemical analyses in order to have a local reference for comparison of Mo and W contents.

3. Analytical methods

Polished sections of queluzite samples were prepared for reflected-light microscopy – i.e., one for each sample, totaling seven (7) polished sections. After investigation using reflected light and reconnaissance energy-dispersive spectroscopy (EDS), sites were selected for electron-microprobe work by means of two electron-probe microanalysers, a Cameca SX100 with tungsten filament and a Cameca SXFiveFE with field emission, at the Technische Universität Clausthal. Wavelength-dispersive-spectroscopy (WDS) measurements were performed using the SXFiveFE instrument at 10 kV and minimum spot size (~100 nm). Reference materials and X-ray emission lines (in parentheses) were as follows: molybdenite (S$K\alpha$ and Mo$L\beta$), rhodonite (Mn$K\alpha$) and pure metal (W$M\alpha$). Counting times were 10 s on peak positions and 5 s on each background. Detection limits, in mass per cent (%), were 0.08% for S, 0.4% for Mn, 0.7% for Mo and 0.07% for W.

Molybdenum and W also had their whole-rock concentrations determined by inductively coupled plasma–mass spectrometry (ICP–MS). The queluzite samples, from which polished sections were prepared, together with two samples of graphite schist, were ground in an agate mill. Their rock powders were submitted to Bureau Veritas Commodities Canada Ltd., Vancouver, for ICP–MS analyses for Mo and W following, respectively, aqua-regia digestion and lithium-borate fusion.

4. Results

Molybdenite is an accessory mineral in the Morro da Mina queluzite. The mineral is present in all samples of queluzite (n = 7), in spatial association with graphite, which is found as disseminations in the rock matrix and also as inclusions in alabandite (Fig. 2a). Reconnaissance EDS work indicated that alabandite has Fe as a minor component – i.e., Fe-bearing MnS. The rock matrix has Mn-rich carbonate and spessartine as predominant components. Ore minerals, of which graphite and alabandite are the most abundant, comprise between about 15 and 25% of the rock. Graphite occurs as platelets as long as 30 μm, whereas alabandite forms aggregates reaching over 500 μm in length; where disseminated, grains of alabandite are generally <50 μm across. The relationship between molybdenite and graphite is best displayed where both minerals are included in alabandite (Fig. 2b). Molybdenite and graphite commonly form sandwich-like aggregates, commonly <30 μm in length, in which a molybdenite platelet is enclosed in a graphite flake (Fig. 2c). Molybdenite platelets are also located on the surface of graphite and in its immediate vicinity (Fig. 2b, c).

Electron-microprobe analyses of molybdenite gave W contents of up to 21%. The results, reported in Table 1, refer to molybdenite grains from one queluzite sample. Table 1 also shows the analyses expressed as percentages of end-member components – i.e., MoS_2, WS_2 and MnS_2. Tungsten-rich domains are indistinguishable under reflected light and backscattered-electron imaging from W-poor molybdenite – i.e., close to the detection limit of 0.07% W. No inclusions of W-rich minerals could be resolved at the scale of observation. Reconnaissance EDS

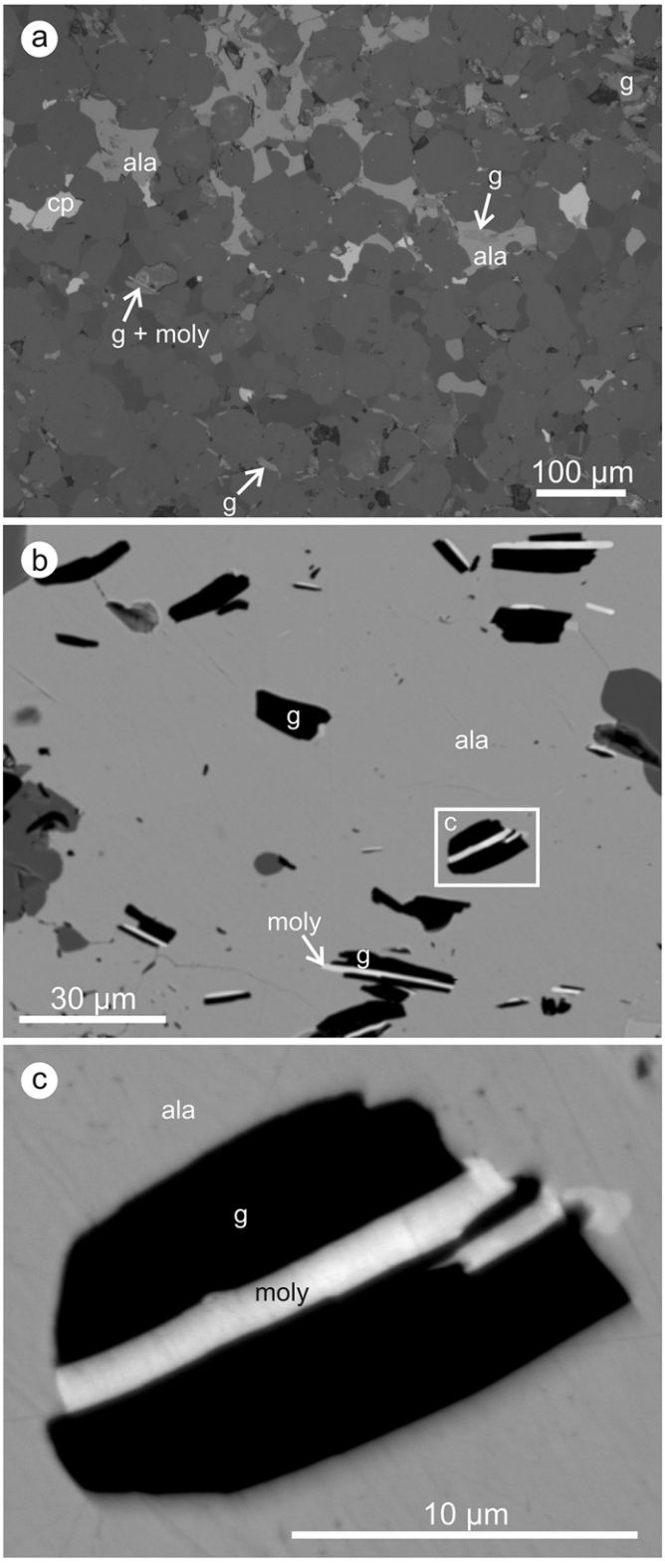

Fig. 2. a. Reflected-light photomicrograph of typical queluzite, in which graphite (g) with and without molybdenite (moly), alabandite (ala) and subordinate sulfide minerals, such as chalcopyrite (cp), are disseminated in a Mn-silicate–carbonate matrix (shades of dark grey). b. Backscattered-electron (BSE) image showing aggregates of graphite and molybdenite (containing WS_2 in solid solution) as inclusions in alabandite. c. Detail of the area marked in b: BSE image of a sandwich-like aggregate of graphite and molybdenite.

Table 1
Representative electron-microprobe analyses of molybdenite intergrown with graphite, Morro da Mina queluzite.

Spot no.	(%, mass)					(mol.%)		
	S	Mn	Mo	W	Total	MnS_2	MoS_2	WS_2
1	37.86	1.73	49.45	12.67	101.70	5.1	83.7	11.2
2	39.03	1.99	55.02	4.79	100.83	5.7	90.2	4.1
3	38.96	1.59	56.48	1.21	98.23	4.6	94.3	1.1
4	36.92	1.81	47.84	11.62	98.19	5.6	83.8	10.6
5	37.25	1.71	46.29	14.11	99.36	5.3	81.7	13.0
6	41.15	2.13	59.74	0.57	103.59	5.8	93.7	0.5
7	40.03	1.71	56.81	3.13	101.66	4.9	92.5	2.7
8	37.01	2.14	42.32	20.90	102.37	6.6	74.3	19.2
9	37.01	1.93	46.64	14.69	100.28	5.9	80.9	13.3
10	40.85	1.71	58.17	0.30	101.03	4.9	94.9	0.3
11	35.84	2.31	44.58	17.17	99.90	7.0	77.4	15.6
12	39.98	1.95	58.81	0.12	100.86	5.5	94.4	0.1
13	38.75	1.64	57.59	0.53	98.51	4.7	94.8	0.5
14	39.10	2.24	56.99	0.49	98.81	6.4	93.2	0.4

work did not reveal any other element than those analysed for in the subsequent WDS session; Ca and Sn, if any, are in trace-element concentrations that could not be detected by means of EDS.

The elements Mo and W are inversely correlated in the queluzite molybdenite, defining a tight array along the MoS_2–WS_2 join (Fig. 3a). This array indicates solid solution of up to 19 mol.% WS_2, the highest amount so far documented in natural molybdenite. It is unlikely that the linear array is caused by interference from inclusions that are invisible at the resolution of the electron microprobe, or from the surrounding material. The latter might be the case for Mn, which yields no significant correlation between Mo and Mn (Fig. 3b).

Whole-rock contents of Mo and W in queluzite vary from 21 to 185 ppm and from 5 to 43 ppm, respectively (Table 2). These results agree with the findings, by reflected-light microscopy, of molybdenite in all queluzite samples. Two samples of graphite schist have lesser amounts of Mo (14–15 ppm) and W (~5 ppm).

Table 2
Whole-rock chemical analyses for Mo and W in queluzite (samples 1–6) and graphite schist (samples 8–9).

Sample no.	Mo (ppm)	W (ppm)
1	67	43
2	84	30
3	29	6.7
4	92	15
5	185	25
6	21	9.9
7	23	4.9
8	14	4.6
9	15	5.1

5. Discussion

5.1. Origin of molybdenite

The close spatial association between molybdenite and graphite, which typically forms sandwich-like aggregates (Fig. 2c), links Mo and S with organic matter in a reducing sedimentary milieu (see below). The nature of the molybdenite–graphite aggregates is that of syntaxial intergrowth, an oriented intergrowth, being {0001} the plane of contact between graphite and molybdenite. Both minerals have the same crystal class and space group. A magmatic-hydrothermal origin for the queluzite molybdenite could be evoked, as molybdenite occurs in intrusion-related ore deposits. However, molybdenite is not concentrated in veins, but it is characteristically disseminated in the rock together with graphite.

The ubiquitous molybdenite–graphite syntaxial intergrowth seems to have resulted from the metamorphism of a precursor rich in organic matter with some S and Mo. Such a precursor is suitably explained by the Mo-trapping capacity of S-rich marine organic matter (e.g., Helz et al., 1996; Tribovillard et al., 2004). In oxygenated seawater, Mo is soluble as molybdate and conservatively remains in solution unless the molybdate ion is converted to particle-reactive thiomolybdate in sulfidic seawater, from which Mo can then be scavenged by sulfidised organic particles, leading to its concentration in black shales (Helz et al., 1996). We thus suggest that the molybdenite disseminated in queluzite is the metamorphic expression of S- and Mo-bearing organic matter that accumulated in a black-shale environment.

5.2. Tungsten-bearing molybdenite as palaeoenvironmental indicator

Like Mo, W not only forms thiotungstate in sulfidic waters (Mohajerin et al., 2014, 2016), but it is also enriched, even though to a much lesser extent than Mo, in sulfide-rich layers hosted in black shales.

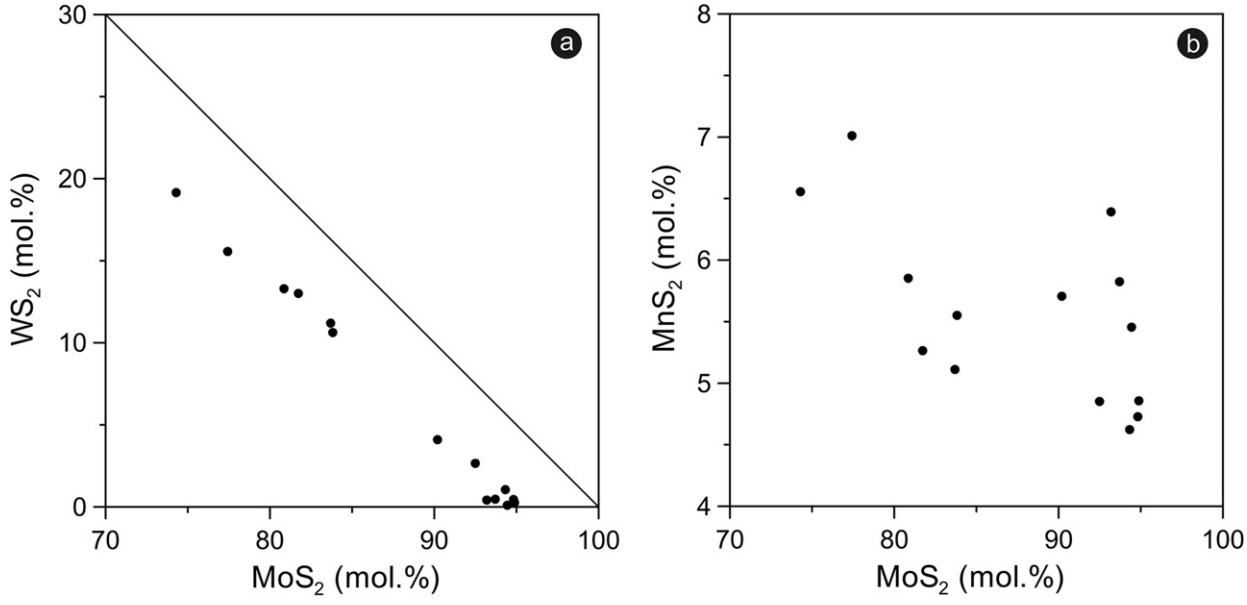

Fig. 3. Diagrams of Mo vs. W (a) and Mo vs. Mn (b), as end-member disulfides, in molybdenite intergrown with graphite (data from Table 1).

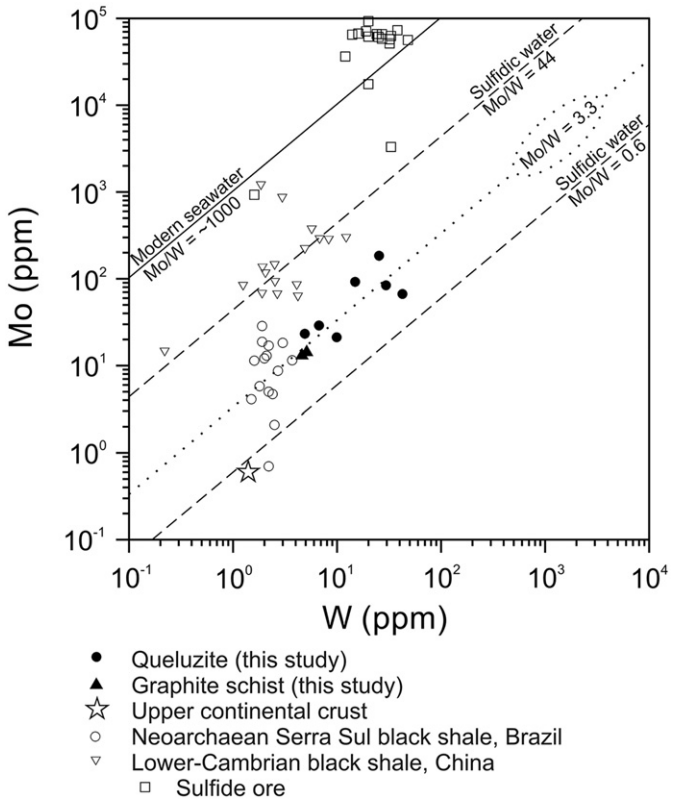

Fig. 4. Diagram of W vs. Mo for queluzite and graphite schist from Morro da Mina, in comparison with the upper continental crust (Hu and Gao, 2008), Neoarchaean black shale (Cabral et al., 2013), Lower-Cambrian sulfide ore and host black shale (Xu et al., 2013), as well as mass Mo/W ratios for seawater (Firdaus et al., 2008), sulfidic pore waters with up to 100 μM H_2S that have mass Mo/W ratios between 0.6 and 44 (Mohajerin et al., 2016), and fluvial and ground waters that show mass Mo/W ratios similar to their basalt country rock – i.e., 3.3 (Arnórsson and Óskarsson, 2007). The mass Mo/W values of the Morro da Mina queluzite and graphite schist and those of the Serra Sul black shale suggest a Mo/W ratio for Archaean seawater that was predominantly derived from weathering of basalt under oxidative conditions.

For example, W contents are on average three orders of magnitude less than Mo in polymetallic sulfide layers hosted in Early-Cambrian black shale in southern China (Xu et al., 2013). Both Mo and W behave conservatively in seawater, the mass Mo/W ratio of which is ~1000 (Firdaus et al., 2008). Assuming that the mass Mo/W ratio of modern seawater is similar to that in the Early Cambrian, mass Mo/W ratios of the aforementioned polymetallic sulfide layers suggest that Mo and W were quantitatively scavenged from seawater into organic-matter-rich sediments (Fig. 4). It is thus reasonable to assume that thiomolybdate and thiotungstate were scavenged together by S-rich organic matter from very sulfidic seawater because H_2S concentrations for thiotungstate formation are two orders of magnitude higher than those required for thiomolybdate (Mohajerin et al., 2016). This is to say that thiotungstate formation and scavenge by organic matter demand considerably higher fS_2/fO_2 ratio than thiomolybdate scavenging. It is pertinent to note that: (i) the mass Mo/W ratios of queluzite and graphite schist are between those, 0.6 and 44 (Fig. 4), for sulfidic pore waters with up to 100 μM H_2S in a present-day estuarine environment (Mohajerin et al., 2016); (ii) the mass Mo/W ratios of queluzite and graphite schist are closer to the average value of fluvial and ground waters, 3.3 (Fig. 4), which is the same as that of their basalt country rock (Arnórsson and Óskarsson, 2007). In both cases, dissolution of Mo- and W-bearing minerals by oxygenated water is implied to account for aqueous molybdate and tungstate.

The finding of Mo enrichment and its correlation with organic carbon in a Neoarchaean black-shale sequence in Western Australia prompted recognition of Mo derivation from seawater containing small amounts of O_2 – that is, the so-called "whiff of oxygen" (Anbar et al., 2007). The reasoning behind the "whiff of oxygen" is that oxidative weathering of molybdenite in crustal rocks is required for mobilising Mo as the unreactive molybdate ion (e.g., Anbar et al., 2007). Likewise, O_2 in the environment would also be demanded for wolframite dissolution and for keeping the tungstate ion soluble in seawater, which needs to be sufficiently oxygenated to prevent formation of Fe and Mn wolframates (e.g., Ryzhenko, 2010).

Applying the considerations above to the molybdenite–tungstenite solid solutions in queluzite, their occurrence indicates: (i) a relatively high fS_2/fO_2 ratio during deposition of the precursor of $(Mo,W)S_2$; (ii) the existence of soluble Mo and W as molybdate and tungstate, respectively, in O_2-bearing seawater above the euxinic water column; (iii) preservation of the high fS_2/fO_2 ratio during subsequent metamorphism. A pristine analogue of the metamorphic molybdenite–graphite intergrowth is a C/MoS_2 mixed-layer phase found in Early-Cambrian black shales of low-grade metamorphism in southern China (Kao et al., 2001).

5.3. Implications for Archaean greenstone belts

The use of Mo enrichment as a proxy for molybdate reduction in a column of anoxic and euxinic waters has relied on sediments and rocks without, or with only low-grade, metamorphic overprint, in which organic C is preserved (e.g., Anbar et al., 2007; Cabral et al., 2013; Dahl et al., 2013; Helz et al., 1996; Lehmann et al., 2007; Tribovillard et al., 2004). These conditions are different from those recorded in the Morro da Mina queluzite, which is hosted in an Archaean greenstone belt that experienced regional metamorphism of amphibolite facies. This raises an important question: how reliable is the Mo proxy in metamorphic rocks where primary organic C is no longer preserved? The expected correlation of Mo enrichment and organic C seems to be expressed as metamorphic $(Mo,W)S_2$–graphite intergrowth that is disseminated in queluzite. Such an intergrowth makes greenstone belts, in particular their graphite-bearing rocks, potential candidates for storing palaeoenvironmental signals in tungstenite-bearing molybdenite that is spatially associated with graphite. Although a precise depositional age for the Archaean Barbacena greenstone belt is not available, the aggregates of graphite and tungstenite-bearing molybdenite are suggestive of a mildly oxygenated water column above anoxic and euxinic waters. Our suggestion is in line with independent evidence that tracks enhanced levels of atmospheric oxygen from 2.5 Ga back to ca. 3.0 Ga ago (Crowe et al., 2013; Stüeken et al., 2015), and of dissolved W in Archaean seawater (Large et al., 2014). The latter is expressed in the low Mo/W ratios recorded in the Morro da Mina queluzite and the Neoarchaean black shale of Serra Sul, Brazil (Fig. 4). Their Mo/W ratios close to those of basalt imply basalt dissolution by O_2-bearing waters (Arnórsson and Óskarsson, 2007).

6. Conclusion

Our study shows that the incorporation of tungstenite into molybdenite as solid solution is more extensive than previously recorded in natural samples. This compositional extension reflects: (i) availability of Mo and W as molybdate and tungstate ions, respectively, in Archaean seawater, (ii) a very high fS_2/fO_2 ratio during the precipitation of $C/(Mo,W)S_2$ from anoxic and euxinic waters; (iii) preservation of the depositional fS_2/fO_2 state during subsequent metamorphic overprint. The new data suggest that $(Mo,W)S_2$–graphite intergrowths might provide a mineralogical proxy for palaeoenvironmental conditions, even for Archaean rocks that experienced regional metamorphism of greenschist and amphibolite facies.

Acknowledgements

VALE is thanked for granting permission to visit and sample the Morro da Mina Mn-ore mine. An anonymous reviewer and Dr Lingang

Xu are gratefully acknowledged for thoughtful comments that greatly improved the manuscript. The expedite editorial handling of Dr Marco Scambelluri is sincerely appreciated.

References

Anbar, A.D., Duan, Y., Lyons, T.W., Arnold, G.L., Kendall, B., Creaser, R.A., Kaufman, A.J., Gordon, G.W., Scott, C., Garvin, J., Buick, R., 2007. A whiff of oxygen before the Great Oxidation Event? Science 317, 1903–1906.

Arnórsson, S., Óskarsson, N., 2007. Molybdenum and tungsten in volcanic rocks and in surface and <100 °C ground waters in Iceland. Geochimica et Cosmochimica Acta 71, 284–304.

Baltazar, O.F., Zucchetti, M., 2007. Lithofacies associations and structural evolution of the Archean Rio das Velhas greenstone belt, Quadrilátero Ferrífero, Brazil: a review of the regional setting of gold deposits. Ore Geology Reviews 32, 471–499.

Barkov, A.Y., Martin, R.F., Poirier, G., Men'shikov, Y.P., 2000. Zoned tungstenoan molybdenite from a fenitized megaxenolith in the Khibina alkaline complex, Kola Peninsula, Russia. Canadian Mineralogist 38, 1377–1385.

Cabral, A.R., Creaser, R.A., Nägler, T., Lehmann, B., Voegelin, A.R., Belyatsky, B., Pašava, J., Seabra Gomes Jr., A.A., Galbiatti, H.F., Böttcher, M.E., Escher, P., 2013. Trace-element and multi-isotope geochemistry of Late-Archean black shales in the Carajás iron-ore district, Brazil. Chemical Geology 362, 91–104.

Candela, P.A., Bouton, S.L., 1990. The influence of oxygen fugacity on tungsten and molybdenum partitioning between silicate melts and ilmenite. Economic Geology 85, 633–640.

Candia, M.A.F., Girardi, V.A.V., 1979. Aspectos metamórficos da Formação Lafaiete em Morro da Mina, distrito de Lafaiete, MG. Boletim IG (Instituto de Geociências, USP). 10, pp. 19–30.

Corrêa Neto, A.V., de Modesto, A.M., Caputo Neto, V., Guerrero, J.C., 2012. Alteração hidrotermal em zona de cisalhamento associada ao Lineamento Congonhas, sul do Quadrilátero Ferrífero, Minas Gerais. Anuário do Instituto de Geociências (UFRJ) 35, 55–64.

Crowe, S.A., Døssing, L.N., Beukes, N.J., Bau, M., Kruger, S.J., Frei, R., Canfield, D.E., 2013. Atmospheric oxygenation three billion years ago. Nature 501, 535–538.

Dahl, T.W., Ruhl, M., Hammarlund, E.U., Canfield, D.E., Rosing, M.T., Bjerrum, C.J., 2013. Tracing euxinia by molybdenum concentrations in sediments using handheld X-ray fluorescence spectroscopy (HHXRF). Chemical Geology 360–361, 241–251.

Dasgupta, S., Banerjee, H., Fukuoka, M., Bhattacharya, P.K., Roy, S., 1990. Petrogenesis of metamorphosed manganese deposits and the nature of the precursor sediments. Ore Geology Reviews 5, 359–384.

Derby, O.A., 1901. On the manganese ore deposits of the Queluz (Lafayette) district, Minas Geraes, Brazil. American Journal of Science 12, 18–32.

Derby, O.A., 1908. On the original type of the manganese ore deposits of the Queluz district, Minas Geraes, Brazil. American Journal of Science 25, 213–216.

Dorr II, J.V.N., 1969. Physiographic, stratigraphic and structural development of the Quadrilátero Ferrífero, Minas Gerais, Brazil. United States Geological Survey Professional Paper 641-A.

Ebert, H., 1957. Beitrag zur Gliederung des Präkambriums in Minas Gerais. Geologische Rundschau 45, 471–521.

Ebert, H., 1962. Baustil und Regionalmetamorphose im präkambrischen Grundgebirge Brasiliens. Tschermaks Mineralogische und Petrographische Mitteilungen 8, 49–81.

Firdaus, M.L., Norisuye, K., Nakagawa, Y., Nakatsuka, S., Sohrin, Y., 2008. Dissolved and labile particulate Zr, Hf, Nb, Ta, Mo and W in the western North Pacific Ocean. Journal of Oceanography 64, 247–257.

Goldschmidt, V.M., 1954. Geochemistry. Oxford University Press.

Grossi Sad, J.H., Pinto, C.P., Duarte, C.L., 1983. Geologia do distrito manganesífero de Conselheiro Lafaiete, MG. Boletim – Núcleo Minas Gerais, Sociedade Brasileira de Geologia 3, 259–270.

Guimarães, D., 1929. Sobre a genese dos minerios de manganez do districto de Lafayette. Annaes da Academia Brasileira de Sciencias 1, 179–182.

Helz, G.R., Miller, C.V., Charnock, J.M., Mosselmans, J.F.W., Pattrick, R.A.D., Garner, C.D., Vaughan, D.J., 1996. Mechanism of molybdenum removal from the sea and its concentration in black shales: EXAFS evidence. Geochimica et Cosmochimica Acta 60, 3631–3642.

Herz, N., Banerjee, S., 1973. Amphibolites of the Lafaiete, Minas Gerais, and the Serra do Navio manganese deposits, Brazil. Economic Geology 68, 1289–1296.

Höll, R., Weber-Diefenbach, K., 1973. Tungstenit-Molybdänit-Mischphasen in der Scheelitlagerstätte Felbertal (Hohe Tauern, Österreich). Neues Jahrbuch für Mineralogie – Monatshefte 27–34.

Hu, Z., Gao, S., 2008. Upper crustal abundances of trace elements: a revision and update. Chemical Geology 253, 205–221.

Hussak, E., 1906. Über die Manganerzlager Brasiliens. Zeitschrift für Praktische Geologie 14, 237–239.

Kao, L.-S., Peacor, D.R., Coveney Jr., R.M., Zhao, G., Dungey, K.E., Curtis, M.D., Penner-Hahn, J.E., 2001. A C/MoS_2 mixed-layer phase (MoSC) occurring in metalliferous black shales from southern China, and new data on jordisite. American Mineralogist 86, 852–861.

Large, R.R., Halpin, J.A., Danyushevsky, L.V., Maslennikov, V.V., Bull, S.W., Long, J.A., Gregory, D.D., Lounejeva, E., Lyons, T.W., Sack, P.J., McGoldrick, P.J., Calver, C.R., 2014. Trace element content of sedimentary pyrite as a new proxy for deep-time ocean–atmosphere evolution. Earth and Planetary Science Letters 389, 209–220.

Lehmann, B., Nägler, T.F., Holland, H.D., Wille, M., Mao, J., Pan, J., Ma, D., Dulski, P., 2007. Highly metalliferous carbonaceous shale and Early Cambrian seawater. Geology 35, 403–406.

Lodders, K., Palme, H., 1991. On the chalcophile character of molybdenum: determination of sulfide/silicate partition coefficients of Mo and W. Earth and Planetary Science Letters 103, 311–324.

Mengason, M.J., Candela, P.A., Piccoli, P.M., 2011. Molybdenum, tungsten and manganese partitioning in the system pyrrhotite–Fe–S–O melt–rhyolite melt: impact of sulfide segregation on arc magma evolution. Geochimica et Cosmochimica Acta 75, 7018–7030.

Miller, B.L., Singewald Jr., J.T., 1917. The manganese ores of the Lafayette district, Minas Geras, Brazil. Transactions of the American Institute of Mining Engineers 56, 7–30.

Moh, G.H., Udubasa, G., 1976. Molybdänit-Tungstenit-Mischkristalle und Phasenrelationen im System Mo–W–S. Chemie der Erde 35, 327–335.

Mohajerin, T.J., Helz, G.R., White, C.D., Johannesson, K.H., 2014. Tungsten speciation in sulfidic waters: determination of thiotungstate formation constants and modeling their distribution in natural waters. Geochimica et Cosmochimica Acta 144, 157–172.

Mohajerin, T.J., Helz, G.R., Johannesson, K.H., 2016. Tungsten–molybdenum fractionation in estuarine environments. Geochimica et Cosmochimica Acta 177, 105–119.

Noce, C.M., Teixeira, W., Quéméneur, J.J.G., Martins, V.T.S., Bolzachini, E., 2000. Isotopic signatures of Paleoproterozoic granitoids from the southern São Francisco craton and implications for the evolution of the Transamazonian orogeny. Journal of South American Earth Sciences 13, 225–239.

Park, C.F.Jr., Dorr II, J.V.N., Guild, P.W., Barbosa, A.L.M., 1951. Notes on the manganese ores of Brazil. Economic Geology 46, 1–22.

Pašava, J., Veselovský, F., Drábek, M., Svojtka, M., Pour, O., Klomínský, J., Škoda, R., Ďurišová, J., Ackerman, L., Halodová, P., Haluzová, E., 2015. Molybdenite–tungstenite association in the tungsten-bearing topaz greisen at Vítkov (Krkonoše–Jizera crystalline complex, Bohemian massif): indication of changes in physico-chemical conditions in mineralizing system. Journal of Geosciences 60, 149–161.

Pašava, J., Svojtka, M., Veselovský, F., Ďurišová, J., Ackerman, L., Pour, O., Drábek, M., Halodová, P., Haluzová, E., 2016. Laser ablation ICPMS study of trace element chemistry in molybdenite coupled with scanning electron microscopy (SEM) – an important tool for identification of different types of mineralization. Ore Geology Reviews 72, 874–895.

Peters, T., Valarelli, J.V., Candia, M.A., 1974. Petrogenetic grids from experimental data in the system Mn–Si–C–O–H. Revista Brasileira de Geociências 4, 15–26.

Pires, F.R.M., 1978. The Archaean Barbacena greenstone belt in its typical development and the Minas itabirite distribution at the Lafaiete district, Minas Gerais. Anais da Academia Brasileira de Ciências 50, 599–600.

Pires, F.R.M., 1983. Manganese mineral parageneses at the Lafaiete district, Minas Gerais, Brazil. Anais da Academia Brasileira de Ciências 55, 271–285.

Ryzhenko, B.N., 2010. Technology of groundwater quality prediction: 1. Eh–pH diagram and detention coefficient of molybdenum and tungsten in aqueous solutions. Geochemistry International 48, 407–414.

Silva, T.P., Figueiredo, M.O., Veiga, J.P., de Oliveira, D., Batista, M.J., Noronha, F., 2015. Tungsten-bearing molybdenite from Borralha. X Congresso Ibérico de Geoquímica, Proceedings, pp. 151–154.

Soares, M.B., Corrêa Neto, A.V., Zeh, A., Cabral, A.R., Pereira, L.F., do Prado, M.G.B., de Almeida, A.M., Manduca, L.G., da Silva, P.H.M., de Mabub, R.O.A., Schlichta, T.M., 2017. Geology of the Pitangui greenstone belt, Minas Gerais, Brazil: stratigraphy, geochronology and BIF geochemistry. Precambrian Research 291, 17–41.

Stüeken, E.E., Buick, R., Anbar, A.D., 2015. Selenium isotopes support free O_2 in the latest Archean. Geology 43, 259–262.

Tribovillard, N., Riboulleau, A., Lyons, T., Baudin, F., 2004. Enhanced trapping of molybdenum by sulfurized marine organic matter of marine origin in Mesozoic limestones and shales. Chemical Geology 213, 385–401.

Viana, N.C. da S., 2009. Mineralogia, calcinação e nova classificação tipológica de minérios de manganês sílico-carbonatados. M.Sc. thesis. Universidade Federal de Ouro Preto, Ouro Preto, Brazil (http://www.repositorio.ufop.br/handle/123456789/3086).

Xu, L., Lehmann, B., Mao, J., 2013. Seawater contribution to polymetallic Ni–Mo–PGE–Au mineralization in Early Cambrian black shales of South China: evidence from Mo isotope, PGE, trace element, and REE geochemistry. Ore Geology Reviews 52, 66–84.